Design and simulation of silicon carbide poly-type double-drift region avalanche photodiodes for UV sensing

ARITRA ACHARYYA[*] , J. P. BANERJEE
Institute of Radio Physics and Electronics, University of Calcutta, 92, APC Road, Kolkata 700009, India.

In this paper the electron and hole dominated photocurrent sensitivity of Double-Drift Region (DDR), p^+-p-n-n^+ structured 4H-SiC Reach-through Avalanche Photodiodes (RAPDs) has been investigated for visible-blind or near visible blind Ultra-Violet (UV) sensing. The photo responsivity and optical gain of the device are obtained by a novel modeling and simulation technique developed by the authors within the wavelength range of 210-350 nm. Two optical illumination configurations of the device such as Top Mounted (TM) and Flip Chip (FC) are considered for the present study to investigate the opto-electric performance of the device separately due to electron dominated and hole dominated photocurrents respectively. Simulation results show that at the wavelength of 260 nm the peak unity gain responsivity and corresponding optical gain are 131 mA/W and 262 respectively for hole dominated photocurrent (i.e in FC structure) while those are 116 mA/W and 208 respectively for electron dominated photocurrent (i.e. in TM structure). Thus better opto-electric performance of 4H-SiC RAPDS can be achieved when the photocurrent is made hole dominated by allowing the light to be incident on the n^+-layer instead of the p^+-layer of the device.

1. Introduction

Reach-through avalanche photodiodes (RAPDs) are already established as high gain and high speed photodetectors. 4H-SiC, a poly-type of SiC having a bandgap of 3.26 eV at 300 K is a suitable base material for APDs for sensing UV light. The advantages of high temperature stability and low leakage current of 4H-SiC devices can be exploited to use this material for realization of high gain-high responsivity detectors in the visible-blind or near visible-blind UV region. Another promising base material for UV sensing is GaN. Although some success has been achieved in the realization of GaN APDs as UV sensor in recent past [1-2], but the performance of detector are limited owing to fabrication issues related to GaN technology. On the other hand SiC is technologically more nature as regards its present state of art and therefore it is a better alternative to GaN as base material of APDs for UV sensing. Further 4H-SiC has additional advantage over GaN as regards its superior thermo-physical properties and marked difference in the ionization rates of electrons (α_n) and holes (α_p) [3] for realizing APDs to have low excess avalanche noise [4-5]. Yan *et al.* [6] experimentally demonstrated the photo-detection capability of p^+-p-n^--n^+ structure of 4H-SiC RAPDs for the first time in 2000. They experimentally obtained peak responsivity of 106 A/W and corresponding optical gain of about 500. Later in 2003, Ng *et al.* [7] experimentally investigated the non local impact ionization effects in 4H-SiC APDs within the wave length range of 230-375 nm. Measurements were carried out on two types of structures

(p^+-p-i-n-n^+ and p^+-p-i-n-n^--n^+) and the experimental results were interpreted by using a simple quantum efficiency model and a non local multiplication theory. They obtained a peak unity gain responsivity more than 130 mA/W at 265nm.

Several analytical and numerical simulation studies on homo-junction and hetero-junction APDs are reported by different researchers [8-13]. But so far as authors' knowledge is concerned no experimental or theoretical verification is available in published literatures till date investigating the effect of electron dominated and hole dominated photo currents separately on the opto-electric performance of avalanche photo diodes in UV range. In the present paper the authors have carried out simulation experiment on DDR, p^+-p-n-n^+ structured 4H-SiC RAPDs for two types of device orientations used to illuminate the device with UV light to investigate the photo-sensitivity and optical gain of the device. Simulation is carried out to investigate the electric and opto-electric performance of UV reach-through APDs (RAPDs) based on 4H SiC for the following two illumination configurations: (a) light is incident on back n^+-layer of the device (i.e. TM structure) and (b) light is incident on top p^+-layer of the device (i.e. FC structure). In the first configuration, (a) the hole component of photo current dominates over the electron component while in the second one (b) the electron component of photo current dominates over hole component. The sensing and photo detecting properties of 4H-SiC DDR RAPDs under both types of optical illumination configurations have been compared in this paper and the superior configuration is suggested.

2. Important Material Parameters of 4H SiC

The gain and responsivity of DDR RAPDs based on 4H-SiC are sensitive functions of electric field (ξ). Field variations of electron and hole ionization rates (α_n and α_p) in 4H-SiC which is given by:

$$\alpha_n(\xi)=\left(\frac{\xi}{A_n}\right)exp\left(\frac{-B_n}{\xi^2}\right) \text{ and } \alpha_p(\xi)=\left(\frac{\xi}{7}\right)exp\left(\frac{-1}{\left(A_p\xi^2+B_p\xi\right)}\right) \text{ (1)}$$

where the values of the constants $A_{n,p}$ and $B_{n,p}$ for a wide electric field range in 4H-SiC are taken from experimentally reported data [3] and listed in Table 1. The electric field dependences of electron and hole drift velocities (v_n and v_p) in 4H-SiC are given by [14]:

$$v_n(\xi)=\left[\frac{\mu_n\xi}{1+\left(\frac{\mu_n\xi}{v_{sn}}\right)^\kappa}\right]^{\frac{1}{\kappa}} \text{ and } v_p(\xi)=\left[\frac{\mu_p\xi}{1+\left(\frac{\mu_p\xi}{v_{sp}}\right)^\kappa}\right]^{\frac{1}{\kappa}} \text{ (2)}$$

where v_{sn} and v_{sp} are the saturation drift velocities of charge carriers and μ_n and μ_p are the carrier mobilities. The value of the constant, $\kappa = 1.20$. The material parameters of 4H-SiC used in the present study are listed in Table 1, while the necessary optical parameters like absorption coefficient ($\alpha(\lambda)$ m^{-1}) and reflectance ($R(\lambda)$) for the wave length range of 210 nm – 350 nm are taken from [15].

Table 1. Material parameters at room temperature (i.e. 300 K)

PARAMETER	VALUE
Bandgap, E_g (eV)	3.26
Ionization coefficient of electrons, A_n (V)	10.00
Ionization coefficient of electrons, B_n ($\times 10^{17}$ V^2/m^2)	4.2680
Ionization coefficient of holes, A_p ($\times 10^{-18}$ m^2/V^2)	4.1915
Ionization coefficient of holes, B_p ($\times 10^{-10}$ m/V)	4.6428
Saturation drift velocity of electrons, v_{sn} ($\times 10^5$ m/s)	2.1200
Saturation drift velocity of holes, v_{sp} ($\times 10^5$ m/s)	1.0800
Mobility of electrons, μ_n ($\times 10^{-1}$ m^{2}V/s)	1.0000
Mobility of holes, μ_p ($\times 10^{-1}$ m^{2}V/s)	0.1000
Dielectric Constant, ε_r	8.5884
Breakdown Electric Field, ξ_c ($\times 10^7$ V/m)	30.00
Thermal Conductivity, k_c (W m^{-1} K^{-1})	490
Electron Diffusion Length, L_n (μm)	1.80
Hole Diffusion Length, L_p (μm)	1.00
Electron Diffusion Coefficient, D_n ($\times 10^{-3}$ m^2 s^{-1})	2.200
Hole Diffusion Coefficient, D_p ($\times 10^{-3}$ m^2 s^{-1})	0.300

3. The device model used for design and simulation

A cross sectional view of DDR 4H-SiC RADPs is shown in Fig. 1 (a) and (b) respectively for two different optical illumination configurations. In the first case (Fig. 1(a)), light is incident on the top p^+-layer so that the photocurrent due to electrons dominate over that of holes (i.e. TM structure) and in the second case (Fig 1 (b)), light is incident on the back n^+-layer so that photocurrent due to holes dominate over that of electrons (i.e. FC structure). The doping levels of the p- and n-layers are designed such that both the layers are totally depleted leading to reach-through structures. Total depletion of p- and n-layers leads to improvement of the impulse response of RAPDs due to

negligible diffusion photocurrent [16] in the active layer of the device. Also the reach through structure of avalanche photo diodes (RAPDs) improves the responsivity of the device and ensures carrier multiplication without excess noise for a specific thickness of multiplication region within the device [16]. Fig. 2 shows the schematic diagram of a DDR RAPD and its typical doping profile. Four different structures of DDR 4H-SiC RAPDs are designed with different doping levels of p- and n-epitaxial layers to study the effect of the level of doping on the opto-electric characteristics of the device. The thickness and doping concentration of different layers are shown in Table 2. The device junction area is taken as $A_j = 200$ μm × 200 μm and the illumination area of the device is taken as $A = 60$ μm × 60 μm.
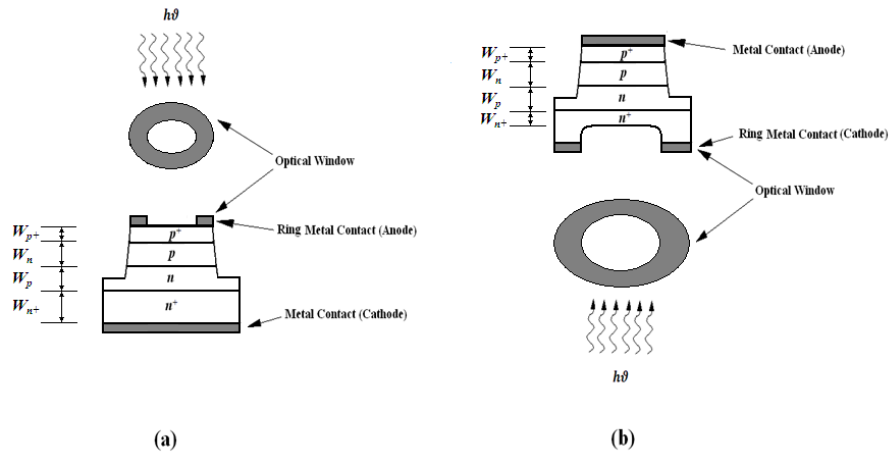
Fig. 1. Cross-sectional view of the 4H-SiC reach-through DDR avalanche photodiodes for two optical illumination configurations (a) TM structure and (b) FC structure.
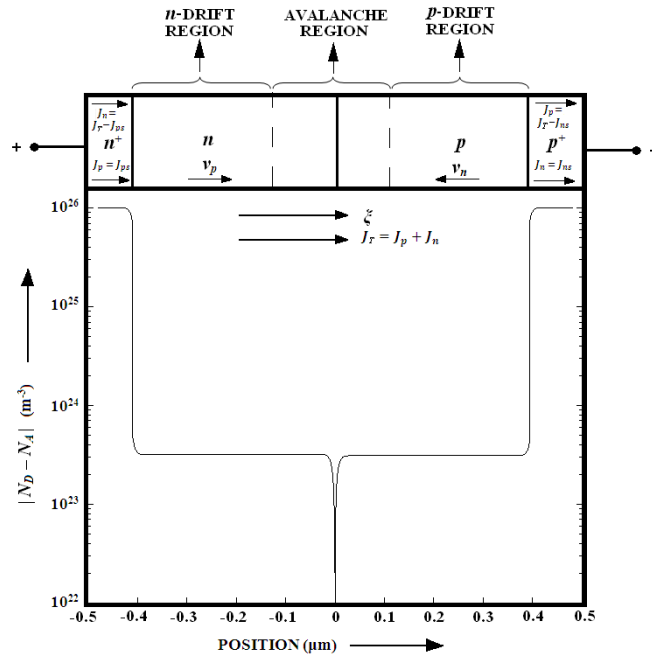
Fig. 2. Schematic of reverse biased DDR RAPD and its doping profile.

Table 2. Design parameters.

Optical Illumination Configuration	Symbol	Thickness of n^+-layer, W_{n+} (µm)	Thickness of p^+-layer, W_{p+} (µm)	Doping concentration of n^+- and p^+-layers, N_{Dn+} and N_{Ap+} ($\times 10^{26}$ m^{-3})	Thickness of n-layer, W_n (µm)	Thickness of p-layer, W_p (µm)	Doping concentration of n-layer, N_D ($\times 10^{23}$ m^{-3})	Doping concentration of p-layer, N_A ($\times 10^{23}$ m^{-3})
TM	RAPD1	0.500	0.150	1.00	0.410	0.395	3.80	3.70
	RADP2	0.500	0.150	1.00	0.410	0.395	3.60	3.50
	RAPD3	0.500	0.150	1.00	0.410	0.395	3.40	3.30
	RADP4	0.500	0.150	1.00	0.410	0.395	3.20	3.10
FC	RAPD1	0.200	0.150	1.00	0.410	0.395	3.80	3.70
	RADP2	0.200	0.150	1.00	0.410	0.395	3.60	3.50
	RAPD3	0.200	0.150	1.00	0.410	0.395	3.40	3.30
	RADP4	0.200	0.150	1.00	0.410	0.395	3.20	3.10

4. Simulation technique

In this section the simulation technique used to investigate the electrical and opto-electrical characteristics of DDR RAPDs is discussed in detail. Using this technique the simulation can be carried out for two different optical illumination configurations i.e. TM and FC structures as mentioned earlier to investigate the electric and opto-electric characteristics of the device under electron dominated and hole dominated photocurrents separately. One-dimensional model of reverse biased p^+-p-n-n^+ structure shown in Fig. 3 is taken for the simulation of DDR RAPDs. The DC electric field and current density profiles in the depletion layer of the device are obtained from simultaneous numerical solution of fundamental device equations i.e., Poisson's equation (equation (3)), combined carrier continuity equation in steady-state (equation (4)), current density equations (equations (5) and (6)) and mobile space charge equation (equation (7)) subject to appropriate boundary conditions (equations (9) and (10)). A double-iterative simulation method developed by the authors is used to solve these above mentioned equations to obtain the electric field and normalized current density profiles. The basic device equations are given by:

$$\frac{d\xi(x)}{dx} = -\frac{d^2V(x)}{dx^2} = \frac{q}{\varepsilon_s}\left(N_D - N_A + p(x) - n(x)\right) \qquad (3)$$

$$\frac{\partial J_n(x)}{\partial x} = -\frac{\partial J_p(x)}{\partial x} = q\left(n(x)\alpha_n(x)v_n(x) + p(x)\alpha_p(x)v_p(x)\right) \quad (4)$$

$$J_n(x) = q\left[v_n(x)\left(1 + \frac{D_n}{v_n(x)}\frac{\partial}{\partial x}\right)\right]n(x) \qquad (5)$$

$$J_p(x) = q\left[v_p(x)\left(1 - \frac{D_P}{v_p(x)}\frac{\partial}{\partial x}\right)\right]p(x) \qquad (6)$$

$$q\frac{\partial(p(x) - n(x))}{\partial x} = \left(J_p(x) + J_n(x)\right)\left(\frac{\alpha_n(x)}{v_n(x)} + \frac{\alpha_p(x)}{v_p(x)}\right) - \left(\alpha_n(x) - \alpha_p(x)\right)\left(\frac{J_p(x)}{v_p(x)} - \frac{J_n(x)}{v_n(x)}\right)$$

$$+ \left[J_p(x)\frac{\partial}{\partial\xi(x)}\left(\frac{1}{v_p(x)}\right) - J_n(x)\frac{\partial}{\partial\xi(x)}\left(\frac{1}{v_n(x)}\right)\right]\frac{\partial\xi(x)}{\partial x} \qquad (7)$$

where N_D and N_A are the donor and acceptor concentrations in n- and p-layers respectively, $p(x)$ and $n(x)$ are respectively the electron and hole concentrations at the space point x, $\xi(x)$ and $V(x)$ are respectively the electric field and potential at x, $J_n(x)$ and $J_p(x)$ are respectively the electron and hole components of total current density ($J_T = J_n(x) + J_p(x)$) at x, q is the electric charge of an electron (1.6×10^{-19} C) and ε_s is the permittivity of the semiconductor material.

Fig. 3. One-dimensional model of DDR APD under two optical illumination configurations i.e. (a) FC structure, (b) TM structure.

The boundary conditions for the electric field at the depletion layer edges are given by:

$$\xi(x = W_{D_n}) = 0 \text{ and } \xi(x = W_{D_p}) = 0 \quad \textit{in FC structure (9 (a))}$$

$$\xi(x = W_{D_p}') = 0 \text{ and } \xi(x = W_{D_n}') = 0 \quad \textit{in TM structure (9 (a))}$$

Similarly the boundary conditions for normalized current density, $P(x) = [(J_p(x) - J_n(x)) / J_T]$ at the depletion layer edges are given by:

$$P(x = W_{D_n}) = \left(\frac{2}{M_p(x = W_{D_n})} - 1\right) \qquad \text{and}$$

$$P(x = W_{D_p}) = \left(1 - \frac{2}{M_n(x = W_{D_p})}\right) \quad \textit{in FC structure} \quad (10 \text{ (a)})$$

$$P(x = W_{D_p}') = \left(1 - \frac{2}{M_n(x = W_{D_p}')}\right) \qquad \text{and}$$

$$P(x = W_{D_n}') = \left(\frac{2}{M_p(x = W_{D_n}')} - 1\right) \quad \textit{in TM structure} \quad (10 \text{ (b)})$$

where $M_n(x)$ and $M_p(x)$ are the position dependent electron and hole multiplication factors [4]. For FC structure (Fig. 3 (a)), the position dependent $M_n(x)$ and $M_p(x)$ can be obtained from the relations given by:

$$M_n(x) = \left[\frac{\exp\left(-\int_{W_{A_n}}^{x}(\alpha_n(x) - \alpha_p(x))dx'\right)}{W_{A_p}^{\int_{W_{A_n}}^{W_{A_p}}\alpha_n(x)\left\{\exp\left(-\int_{W_{A_n}}^{x}(\alpha_n(x) - \alpha_p(x))dx''\right)\right\}dx'}}\right] \qquad (11 \text{ (a)})$$

$$M_p(x) = \left[\frac{\exp\left(-\int_{x}^{W_{A_p}} (\alpha_p(x) - \alpha_n(x))dx'\right)}{\int_{W_{A_n}}^{W_{A_p}} \alpha_p(x) \left\{ \exp\left(-\int_{x'}^{W_{A_p}} (\alpha_p(x) - \alpha_n(x))dx''\right)\right\}dx'} \right] \quad (11\text{ (b)})$$

Similarly when light is illuminated on the p^+-layer (Fig. 3 (b)) of the device, the $M_n(x)$ and $M_p(x)$ can be obtained from the relations given by:

$$M_n(x) = \left[\frac{\exp\left(-\int_{W_{A_p}}^{x} (\alpha_n(x) - \alpha_p(x))dx'\right)}{\int_{W_{A_p}}^{W_{A_n}} \alpha_n(x) \left\{ \exp\left(-\int_{W_{A_p}}^{x'} (\alpha_n(x) - \alpha_p(x))dx''\right)\right\}dx'} \right] \quad (12\text{ (a)})$$

$$M_p(x) = \left[\frac{\exp\left(-\int_{x}^{W_{A_n}'} (\alpha_p(x) - \alpha_n(x))dx'\right)}{\int_{W_{A_p}'}^{W_{A_n}'} \alpha_p(x) \left\{ \exp\left(-\int_{x'}^{W_{A_n}'} (\alpha_p(x) - \alpha_n(x))dx''\right)\right\}dx'} \right] \quad (12\text{ (b)})$$

Assuming that the carrier multiplication occurs only within the avalanche region, it can be concluded that, the electron multiplication factor at the edge of the depletion layer at n-side is same as electron multiplication factor at the edge of the avalanche zone at n-side, i.e.:

$$M_n\left(x = W_{D_n}\right) = M_n\left(x = W_{A_n}\right) \qquad \text{and}$$
$$M_n\left(x = W_{D_n}'\right) = M_n\left(x = W_{A_n}'\right) \qquad (13)$$

Similarly the hole multiplication factor at the edge of the depletion layer at p-side is same as hole multiplication factor at the edge of the avalanche zone in p-side, i.e.:

$$M_p\left(x = W_{D_p}\right) = M_n\left(x = W_{A_p}\right) \qquad \text{and}$$

$$M_p\left(x = W_{D_p}'\right) = M_p\left(x = W_{A_p}'\right) \qquad (14)$$

Electric field profiles and current profiles are obtained from the DC simulation. The applied reverse bias voltage can be obtained by integrating the spatial field profile over the total depletion layer width, i.e.:

$$V_R = \int_{W_{D_n}}^{W_{D_p}} \xi(x)dx \qquad \text{in FC structure} \qquad (15)$$

$$V_R = \int_{W_{D_p}'}^{W_{D_n}'} \xi(x)dx \qquad \text{in TM structure} \qquad (16)$$

If P_{in} watts of optical power is incident on the device having effective device illumination area of A, then the photon flux density Φ_0 is given by:

$$\Phi_0 = P_{in} \frac{(1 - R(\lambda))\lambda}{Ahc} \qquad (17)$$

The electron-hole pair (EHP) generation rate ($G_L(x)$) due to optical illumination is given by:

$$G_L(x) = \Phi_0 \alpha(\lambda) \exp(-\alpha(\lambda)x) = P_{in} \frac{\alpha(\lambda)(1 - R(\lambda))\lambda}{Ahc} \exp(-\alpha(\lambda)x) \quad (18)$$

where $\alpha(\lambda)$ and $R(\lambda)$ are the absorption coefficient (m^{-1}) and reflectance [$R = (n_2 - n_1)/ (n_2 + n_1)$; n_2 = refractive index of the semiconductor, n_1 = refractive index of air] of the semiconductor material respectively at a wavelength of λ.
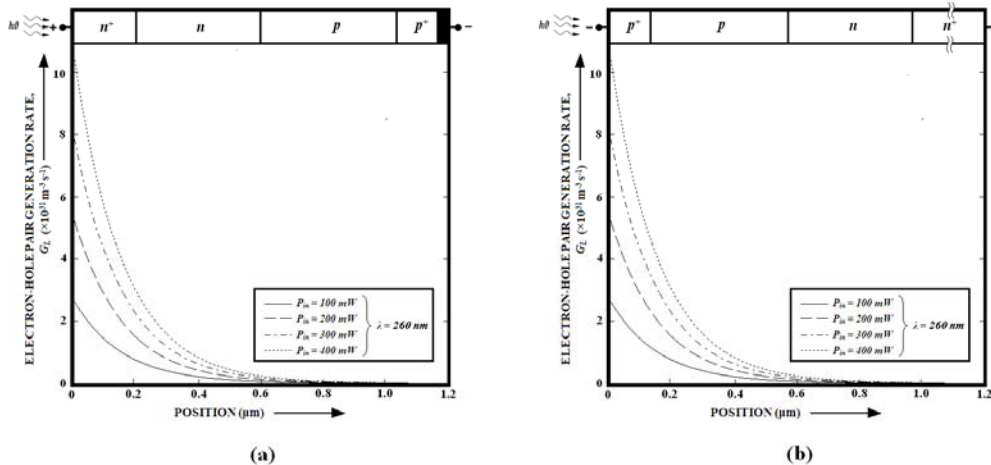
Fig. 4. Carrier generation characteristics in DDR APD (a) FC structure, (a) TM structure.

The electron and hole multiplication factors at the n- and p-depletion layer edges are given by:

$$M_n = \frac{J_T}{J_{ns(Total)}} \qquad \text{and} \qquad M_p = \frac{J_T}{J_{ps(Total)}} \qquad (19)$$

where $J_{ns/ps(Total)}$ is the total electron/hole reverse saturation current under optical illumination. Electron and hole reverse saturation currents can have two components such as (a) thermally generated saturation currents ($J_{ns(Th)}$ and $J_{ps(Th)}$) and (b) optically generated saturation currents ($J_{ns(Opt)}$ and $J_{ps(Opt)}$). Thus:

$$J_{ns(Total)} = J_{ns(Th)} + J_{ns(Opt)} \qquad \text{and}$$

$$J_{ps(Total)} = J_{ps(Th)} + J_{ps(Opt)} \qquad (20)$$

The expression for thermally generated electron and hole reverse saturation currents are given by:

$$J_{ns(Th)} = \left[\frac{q D_n n_i^2}{L_n N_A} \right] \text{ and } J_{ps(Th)} = \left[\frac{q D_p n_i^2}{L_p N_D} \right] \qquad (21)$$

The drift component of the photocurrent density ($J_{ps(Opt\ drift)}$ and $J_{ns(Opt\ drift)}$) through the reverse-biased depletion layer is given by:

$$J_{ps(Opt\ drift)} = -q \int_{W_{D_n}}^{W_{D_p}} G_L(x)dx = qP_{in}\frac{(1-R(\lambda))\lambda}{Ahc}\left\{ exp(-\alpha(\lambda)W_{D_n}) - exp(-\alpha(\lambda)W_{D_p}) \right\}$$

$$\text{in FC structure} \qquad (22)$$

$$J_{ns(Opt\ drift)} = -q \int_{W_{D_p}'}^{W_{D_n}'} G_L(x)dx = qP_{in}\frac{(1-R(\lambda))\lambda}{Ahc}\left\{ exp(-\alpha(\lambda)W_{D_p}') - exp(-\alpha(\lambda)W_{D_n}') \right\}$$

$$\text{in TM structure} \qquad (23)$$

Due to very high conductivity, electric fields at the p^+- and n^+-layers are zero. Diffusion components of the photo current are generated within these undepleted p^+- and n^+-layers. Diffusion components of the photo current in both p^+- and n^+-layers separately can be determined by solving the one-dimensional diffusion equation with proper boundary conditions [17]. The electron and hole diffusion components of the photo current density ($J_{ps(Opt\ diff)}$ and $J_{ns(Opt\ diff)}$) in both p^+- and n^+-layers are given by:

$$J_{ns(Opt\ diff)} = qP_{in}\frac{(1-R(\lambda))\lambda}{A_j hc}\left(\frac{\alpha(\lambda)L_n}{1+\alpha(\lambda)L_n} \right)exp(-\alpha(\lambda)W_{D_p})$$

$$\text{in FC structure} \qquad (24)$$

$$J_{ps(Opt\ diff)} = qP_{in}\frac{(1-R(\lambda))\lambda}{A_j hc}\left(\frac{\alpha(\lambda)L_p}{1+\alpha(\lambda)L_p} \right)exp(-\alpha(\lambda)W_{D_n}')$$

$$\text{in TM structure} \qquad (25)$$

Total photocurrent density is the combination of drift and diffusion components; i.e.:

$$\left. \begin{array}{l} J_{ps(Opt)} = J_{(Opt\ drift)} + J_{ps(Opt\ diff)} \qquad \text{in FC structure} \\ \qquad\qquad \text{and} \\ J_{ns(Opt)} = J_{(Opt\ drift)} + J_{ns(Opt\ diff)} \qquad \text{in TM structure} \end{array} \right\} (26)$$

When the light is shined on the n^+-side of the DDR RAPD device (i.e. FC structure), then the photocurrent density is hole dominated. For this case, the electron and hole multiplication factors at the n- and p-depletion layer edges are given by:

$$M_n(x=W_{D_p}) = \frac{J_T}{J_{ns(Th)}} \text{ and } M_p'(x=W_{D_n}) = \frac{J_T}{J_{ps(Th)} + J_{ps(Opt)}} \qquad (27)$$

In this case the value of M_p' is considerably reduced while M_n remains unchanged. Thus the normalized current density boundary conditions at the depletion layer edges (equation (10 (a))) are modified to:

$$P(x=W_{D_n}) = \left(\frac{2}{M_p'(x=W_{D_n})} - 1 \right) \text{ and } P(x=W_{D_p}) = 1 \text{ in FC structure} \quad (28)$$

where M_n is very large ($\approx 10^6$) near the breakdown of the device and M_p' is much smaller than M_n under similar condition. The equation (28) is used as one of the boundary conditions in the proposed model (in place of equation (10 (a))) for simulating the opto-electric properties of the n^+-layer illuminated DDR RAPD device.

When the light is shined on the p^+-side of the DDR RAPD device, then the photocurrent density will be electron dominated. So the electron and hole multiplication factors at the n- & p-depletion layer edges are given by:

$$M_n'(x=W_{D_p}') = \frac{J_T}{J_{ns(Th)} + J_{ns(Opt)}} \text{ and } M_p(x=W_{D_n}') = \frac{J_T}{J_{ps(Th)}} \qquad (29)$$

In this case the value of M_n' is considerably reduced while M_p remains unchanged. Thus the normalized current density boundary conditions at the depletion layer edges (equation (10 (b))) are modified to:

$$P(x=W_{D_p}') = \left(1 - \frac{2}{M_n'(x=W_{D_p}')} \right) \text{ and } P(x=W_{D_n}') = -1 \text{ in TM structure} \quad (30)$$

where M_p is very large ($\approx 10^6$) ner the breakdown of the device and M_n' is much smaller than M_p under similar condition. The equation (30) is used as one of the boundary conditions in the proposed model (in place of equation (10 (b))) for simulating the opto-electric properties of the p^+-layer illuminated DDR RAPD device.

Total primary unmultiplied photocurrent (I_{ph}) can be written as:

$$I_{ph} = (J_{ps\_opt} + J_{ns\_opt})A_j \qquad (31)$$

Total multiplied photocurrent (I_M) is given by:

$$I_M = (M_p J_{ps\_opt} + M_n J_{ns\_opt})A_j \qquad (32)$$

In the avalanche phenomenon of reverse biased DDR APDs both electrons and holes participate; a mean value of avalanche multiplication factor can be expressed as:

$$M = \frac{I_M}{I_{ph}} = \frac{(M_p J_{ps\_opt} + M_n J_{ns\_opt})}{(J_{ps\_opt} + J_{ns\_opt})} \qquad (33)$$

The responsivity $\Re$ (A/W) of an APD is defined as the output photocurrent per unit incident optical power:

$$\Re = \frac{I_M}{P_{in}} = M\frac{I_{ph}}{P_{in}} = M.\Re_{unity\_gain} \qquad (34)$$

5. Results and discussion

A double-iterative computational method is used by the authors to carry out the simulation as discussed in the previous section. Simulation is carried out to study the electrical and opto-electrical characteristics of the designed DDR 4H-SiC RAPDs (Table 2). Simulated electric field profiles are shown in Fig. 5 near breakdown voltages under dark condition. Breakdown voltages of RAPD1, RAPD2, RAPD3 and RAPD4 are calculated by integrating the electric field profiles within the entire depletion regions of the corresponding devices. Breakdown voltages of RAPD1, RAPD2, RAPD3 and RAPD4 are obtained as 159.3 V, 160.7 V, 162.9 V and 164.5 V respectively. Breakdown voltage increases as the doping levels of the active layers decreases. Spatial variations of impact ionization rates for electrons (α_n) and holes (α_p) in DDR 4H-SiC RAPDs are shown in Fig. 6. It is interesting to observe that the ionization rate of holes (α_p) is higher compared to the ionization rate of electrons (α_n) at each space points within the active region of the device. Also both α_p and α_n are higher at each space points within its low field regions in RAPDs with lower doping levels, because at low field regions electric fields at each space point is higher for lower doping level RAPDs. But at high field regions α_p and α_n associated with different RAPDs do not differ much, because at high-field regions electric fields at each space points are very close to each other for all the RAPDs under consideration.
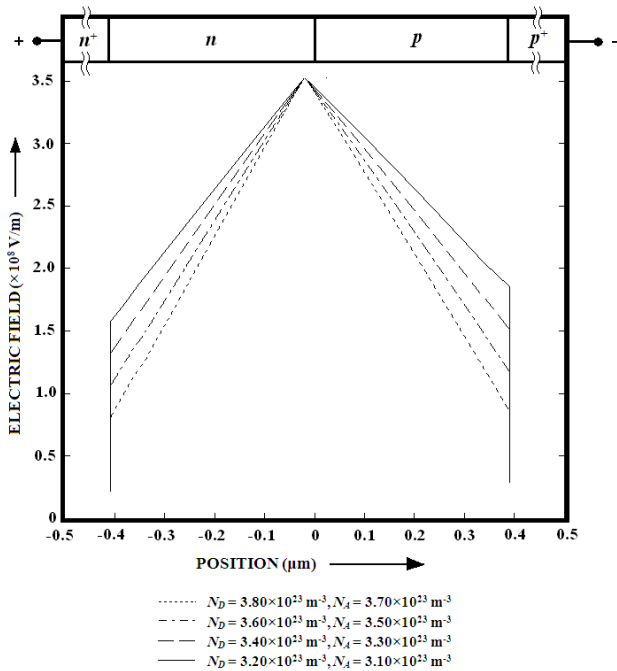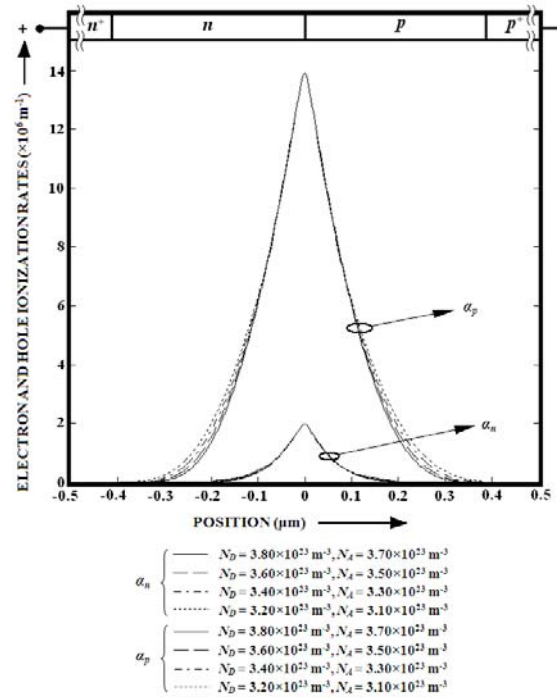
Fig. 6. Spatial variations of electron and hole ionization rates in unilluminated DDR 4H-SiC RAPDs near breakdown.

Now the effect of optical illumination on the electric field profile of the device is investigated for two different optical illumination configurations. Fig. 7 shows that change in electric profile of RAPD2 when optical power (P_{in}) of 100, 200 and 300 mW of 260 nm wavelength is incident of the n^+-layer of RAPD2. Since the optical energy is incident on the n^+-layer, electron-hole pair (EHP) generation rate at the starting of the n^+-layer is highest and it exponentially decays to zero nearly at the middle of the p-layer (Fig. 4(a)). That is why the distortion of electric field at each space points within the n-layer is higher compared to the p-layer. Also this distortion is larger when incident optical power is higher. But totally opposite effect is observed when light is illuminated on the p-layer (referred to Fig. 4 (b))), i.e. the distortion of electric field at each space point is higher within p-layer (Fig. 8). It is interesting to observe that, distortion of electric field is greater when light is illuminated on n^+-layer, i.e. when photo current is hole dominated (FC structure) as compared to when light is illuminated on p^+-layer, i.e. when photo current is electron dominated (TM structure). It is occurred, because the ionization rate of holes (α_p) is higher than that of electrons (α_n) in 4H-SiC [3]; that is why 4H-SiC based APDs are more sensitive to hole dominated photocurrent. This effect is similar as InP based avalanche transit time (ATT) devices [18] where $\alpha_p > \alpha_n$, but opposite of Si based ATT devices [19-20] where $\alpha_n > \alpha_p$. Multiplication factors are plotted against reverse bias voltages for both type of optical illumination configurations for 260 nm wavelength in Fig. 9 and Fig. 10. It is observed that peak multiplication factor is higher for hole dominated photo current (highest 262) compared to that of electron dominated photocurrent (highest 208).

Fig. 5. Simulated Electric Field Profiles of unilluminated DDR 4H-SiC RAPDs near breakdown.

Also multiplication factor is higher for lower doping level RAPDs due to their expected wider avalanche zones or multiplication regions.
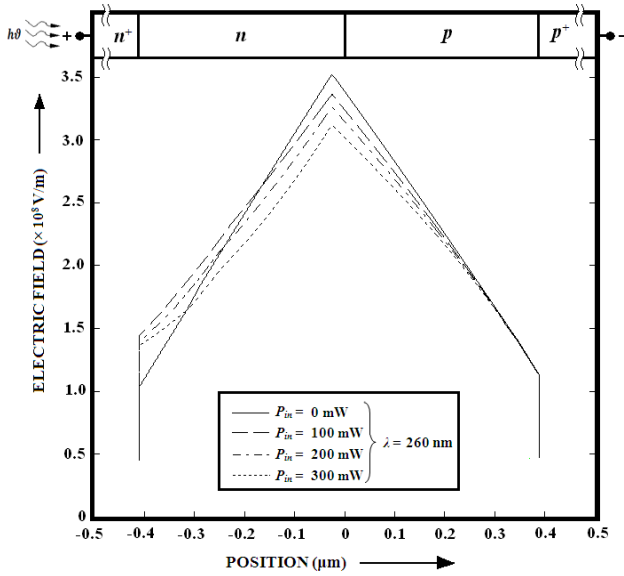
Fig. 7. Variations in Electric Field Profiles of RAPD2 near breakdown due to optical illuminated on the n^+-layer (FC structure).
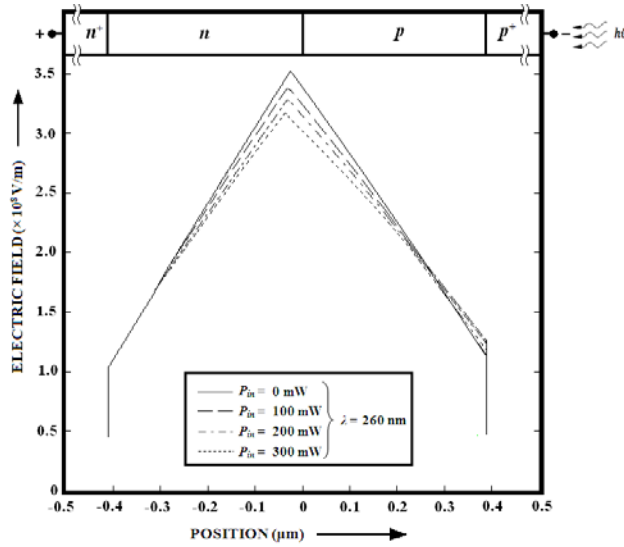
Fig. 8. Variations in Electric Field Profiles of RAPD2 near breakdown due to optical illuminated on the p^+-layer (TM structure).

Unity gain responsivity curves of DDR 4H-SiC APDs are shown in Fig. 11 and Fig. 12 for both types of optical illumination configurations. Unit gain responsivities are calculated for the wavelength 210-350 nm and it is observed that the peak responsivity is obtained at 260 nm wavelength for both types of optical illumination configurations (FC and TM). Peak unity gain responsivities are higher (maximum 131 mA/W at 260 nm in FC structure) for hole dominated photocurrent compared as to electron dominated photocurrent (maximum 116 mA/W at 260 nm in TM structure). It is

also interesting to observe that due to wider avalanche widths, lower doping level RAPDs produces higher photo current due to same amount of incident optical power. It can be noticed from Fig. 11 and Fig. 12 that in both the optical illumination configurations (FC and TM) the device shows unity gain responsivity peaks at 260 nm wavelength which is also observed in the earlier experimental reports on 4H-SiC APDs [6-7].
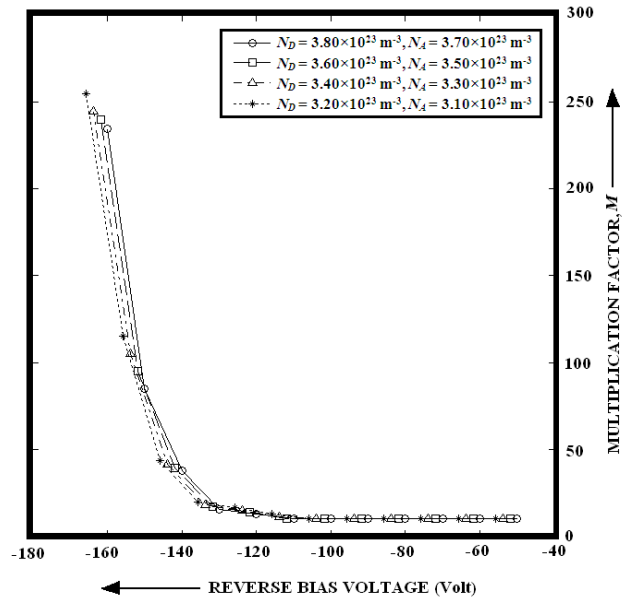
Fig. 9. Variation of Multiplication Factor with Reverse Bias Voltage in DDR 4H-SiC RAPDs due to optical illuminated on the n^+-layer (FC structure).
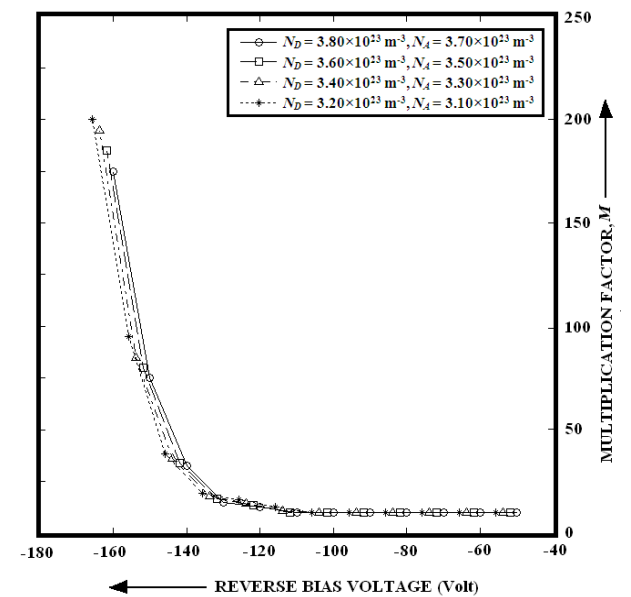
Fig. 10. Variation of Multiplication Factor with Reverse Bias Voltage in DDR 4H-SiC RAPDs due to optical illuminated on the p^+-layer (TM structure).
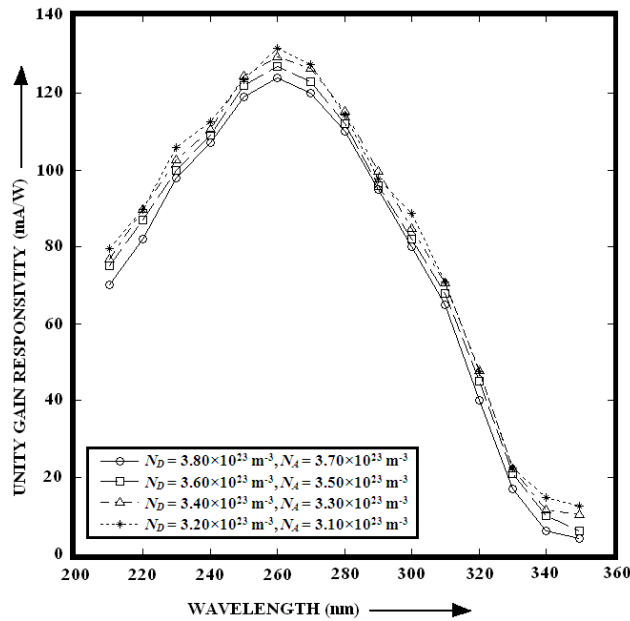
Fig. 11. Variation of Unity Gain Spectral Responsivity with Wavelength in DDR 4H-SiC RAPDs due to optical illuminated on the n^+-layer (FC structure).
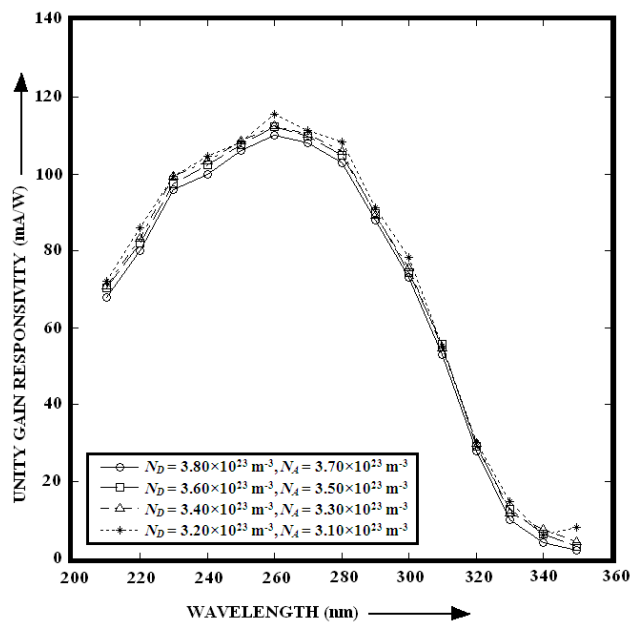
Fig. 12. Variation of Unity Gain Spectral Responsivity with Wavelength in DDR 4H-SiC RAPDs due to optical illuminated on the p^+-layer (TM structure).

6. Validation of the simulation results

B. K Ng *et al.* [7] experimentally investigated the avalanche multiplication and excess noise characteristics of two different structures (p^+-p-i-n-n^+ and p^+-p-i-n-n^--n^+) of 4H-SiC APDs in 2003. A Hg-Xe lamp and a HeCd laser were used as UV source to study the multiplication characteristics of the APDs under different carrier injection conditions. The spectral response of the devices

was measured within the wavelength range of 230-275 nm. They obtained peak unity gain responsivity of the device more than 130 mA/W at 265 nm with multiplication factor higher than 200. The simulation results presented in this paper show that 131 mA/W of peak unity gain responsivity at 260 nm wavelength may be achieved with a multiplication factor of 262 from DDR (p^+-p-n-n^+) 4H-SiC RAPD when the UV light is illuminated on the n^+-layer of the device (i.e. FC structure) in which the photocurrent is hole dominated. Thus the simulation results are in close agreement with the experimentally obtained results of B. K. Ng *et al.* [7]. Slight deviation in the simulation results from the experimental results may be due to the difference in structural and doping parameters of the devices, electrical bias conditions and the intensity of the incident optical power.

7. Conclusions

Electrical and opto-electrical characteristics of 4H-SiC based RAPDs are investigated in this paper within visible-blind and nearly visible-blind UV range (210-350 nm). Results shows that peak unity gain responsivity of 131 mA/W at 260 nm can be achieved with a multiplication factor of 262 when light is illuminated on the n^+-layer of the device, i.e. when the photocurrent is hole dominated (i.e. FC structure). Due to higher hole ionization rate compared to electron ionization rate ($\alpha_p > \alpha_n$) in 4H-SiC, the DDR 4H-SiC RAPDs are more sensitive to hole dominated photocurrent as compared to electron dominated photocurrent. So, it can be concluded that light has to be illuminated on n^+-layer of the device to get better opto-electrical performance of DDR 4H-SiC RAPDs. Results are extremely encouraging to fabricate p^+-p-n-n^+ 4H-SiC RAPDs for high performance visible-blind and nearly visible-blind UV applications.

References

[1] K. A. McIntosh, R. J. Molnar, L. J. Mahoney, A. Lightfoot, M.W. Geis, K. M. Molvar, I. Melngailis, R. L. Aggarwal,W. D. Goodhue, S. S. Choi, D. L. Spears, S. Verghese, Appl. Phys. Lett. **75**, 3485 (1999).
[2] B. Yang, T. Li, K. Heng, C. Collins, S. Wang, J. C. Carrano, R. D. Dupuis, J. C. Campbell, M. J. Schurman, I. T. Ferguson, IEEE J. Quantum Electron. **36**, 1389 (2000).
[3] A. O. Konstantinov, Q.Wahab, N. Nordell, U. Lindefelt, Appl. Phys. Lett. **71**, 90 (1997).
[4] R. J. McIntyre, IEEE Trans. Electron Devices. **13**, 164 (1966).
[5] B. K. Ng, F. Yan, J. P. R. David, R. C. Tozer, G. J. Rees, C. Qin, and J. H. Zhao, IEEE Photon. Technol. Lett. **14**, 1342 (2002).
[6] Feng Yan, Jian H. Zhao, Gregory H. Olsen, Solid State Electronics. **44**, 341 (2000).

[7] B. K. Ng, John P. R. David, Richard C. Tozer, Graham J. Rees, Feng Yan, Jian H. Zhao, Maurice Weiner, IEEE Trans. Electron Devices. **50**, 1724 (2003).

[8] H. Mokari, M. H. Seyedi, Progress In Electromagnetics Research C. **3**, 45 (2008).

[9] H. Mokari, P. Derakhshan-Barjoei, Progress In Electromagnetics Research B. **7**, 159 (2008).

[10] K. Kagawazadeh, IEEE Trans. Electron Devices. **19**, 703 (1972).

[11] R. B. Emmons, J. Appl. Phys. **38**, 3705 (1967).

[12] J. C. Campbell, S. Chandrasekhar, W. T. Tsang, G. J. Qua, B. C. Johnson, J. Lightwave Technol. **7**, 473 (1989).

[13] G. E. Stillman, C. M. Wolfe, in Semiconductors and Semimetals, R. K. Willardson and A. C. Beer, Eds. New York: Academic, **12**, 291 (1977).

[14] K. V. Vassilevski, K. Zekentes, A. V. Zorenko, L. P. Romanov, IEEE Electron Device Letters. **21**, 485 (2000).

[15] "Electronic Archive: New Semiconductor Materials, Characteristics and Properties," http://www.ioffe.ru/SVA/NSM/ Semicond/SiC.

[16] J. M. senior, Optical Fiber Communications: Principles and Practice, Pearson Education: 2nd Edition, India (2007).

[17] S. M. Sze, Kwok K. Ng, Physics of Semiconductor Devices, Willy-India: 3rd Edition, India (2010).

[18] J. P. Banerjee, R. Mukherjee J. Mukherjee, P. N. Mallik, Phys. Stat. Sol. (a). **153**, 567 (1996).

[19] H. P. Vyas, R. J. Gutmann, J. M. Borrego, IEEE Transactions on Electron Devices. **26**, 232 (1979).

[20] A. Acharyya, J. P. Banerjee, Iranian Journal of Electrical & Electronic Engineering, **7**, 179 (2011).

_____
[*]Corresponding author: ari_besu@yahoo.co.in